Colloid Polym Sci 278:469–474 (2000)

SHORT COMMUNICATION

T. Okubo
H. Yoshimi
T. Shimizu
R. H. Ottewill

Giant colloidal crystals of fluorine-containing polymer spheres in exhaustively deionized aqueous suspensions and in the presence of sodium chloride

Received: 27 October 1999
Accepted in revised form: 16 November 1999

T. Okubo (✉) · H. Yoshimi
Department of Applied Chemistry
Faculty of Engineering, Gifu University
Yanagido 1-1, Gifu 501-1193, Japan
e-mail: okubotsu@apchem.gifu-u.ac.jp
Fax: +81-58-2932628

T. Shimizu
Daikin Industries Co., Settsu
Osaka 566-8585, Japan

R. H. Ottewill
School of Chemistry
University of Bristol Cantock's Close
Bristol BS8 1TS, UK

Abstract Gigantic colloidal single crystals (2–6 mm) are formed for fluorine-containing polymer spheres (120–210 nm in diameter) in exhaustively deionized aqueous suspensions. The spheres used are poly(tetrafluoroethylene) (PTFEA and PTFEB), copolymer of tetrafluoroethylene and perfluorovinylether (PFA) and copolymer of tetrafluoroethylene and perfluoropropylene (PTP). The phase diagrams of these spheres are obtained in the deionized suspensions and also in the presence of sodium chloride for PFA. The critical sphere concentrations of crystal melting (ϕ_c) for these spheres are around 0.0006 in volume fraction, which are close to, but slightly larger than, those of monodispersed polystyrene spheres ($\phi_c \approx 0.00015$) and colloidal silica spheres(ϕ_c = 0.0002–0.0004) reported previously. The crystals are largest when the sphere concentrations are a bit higher than the ϕ_c value and their size decreases as the sphere concentration increases. Reflection spectra are taken in sedimentation equilibrium as a function of the height from the bottom of the suspension. The static elastic modulus is estimated to be 10.8 and 28.7 Pa for PTFEA and PTP spheres at the sphere concentrations 0.00325 and 0.00322 in volume fraction, respectively.

Key words Colloidal crystal · Fluorine-containing polymer · Giant crystals · Morphology · Reflection spectra

Introduction

Recently, keen attention has been paid to the structural and dynamic properties of colloidal crystals [1–13]. The colloidal crystals studied so far are grouped into "soft" crystals in dilute and deionized aqueous suspensions [14–16] and "hard" crystals in concentrated suspensions in refractive-index-matched organic solvents [17–21].

We must pay great attention to the complete deionization of the suspension for aqueous soft systems. The critical sphere concentration of melting (ϕ_c) is quite sensitive to the degree of deionization of the suspension and increases sharply for suspensions contaminated with ionic impurities. When the sample suspensions are deionized with ion-exchange resins for a long time, more than several months, for example, the ϕ_c value becomes quite low and ranges from 0.0001 to 0.0004 irrespective of the kind of spheres (100–130 nm in diameter) [22–24]. Very large single crystals (8 mm in the largest case) have been observed when the sphere concentrations are close to the ϕ_c value and the suspension has been deionized exhaustively. The size of the single crystals increased sharply when the sphere concentration decreased. These observations are quite understandable because crystal size should increase with decreasing nucleation rate and also with decreasing number of nuclei. The nucleation rate decreases as the sphere concentration decreases. When the sphere concentration is high ($\phi > 0.01$), the crystals are very small (around 0.02 mm or smaller) and are not observed with the naked eye. It should be noted here that all the single crystals are surrounded by grain boundaries and are packed densely throughout the suspension.

As has been firmly clarified, colloidal crystals are formed by the intersphere repulsion forces, which in turn favour entropically driven ordering in a closed vessel. An essential part of the repulsion is from the translational Brownian (thermal) movement of the colloidal spheres themselves. Sizes of colloidal spheres ranging from 80 to 200 nm are appropriate for forming a crystal-like distribution of spheres in water at room temperature. Spheres smaller than 80 nm move much more vigorously to form crystal-like structures. This situation is understood by the fact that nitrogen molecules, for example, which are much smaller than the colloidal size, never crystallize at room temperature.

Generally speaking, colloidal spheres have negative charges on their surfaces. Furthermore, many very small simple ions are oppositely charged and are distributed around the negatively charged large spheres called "electrical double layers". In the deionized state, the double layers are very thick and the electrostatic intersphere repulsive forces prevail to a distance as far as micrometres. Thus, colloidal crystallization in the deionized aqueous suspension takes place quite easily at very low sphere concentrations compared with the sphere systems including no electrostatic intersphere repulsion besides that from Brownian movement of spheres. Quite recently Itano et al. [25] reported that Coulomb crystals are formed for trapped spherical plasmas with a single sign(plus) of charge in the gas phase. This observation supports strongly the important role of the electrostatic repulsion forces for the crystallization besides Brownian movement of the respective plasmas.

Polystyrene and colloidal silica spheres have often been used for studies on colloidal crystallization. The former are hydrophobic in water and apt to aggregate especially at the interfaces with air and/or cell walls, whereas the latter are strongly hydrophilic and do not aggregate. The fluorine-containing colloidal spheres studied in this work are strongly hydrophobic; therefore, great attention was paid to prevent aggregation by minimizing the contact area of the suspension with air and/or cell walls and by preventing the agitation of the suspension. As described later, this work clarifies that colloidal crystallization takes place irrespective of the hydrophobicity of the colloidal spheres. This is due to the fact that the short-ranged hydrophobic interaction is negligible compared with the intersphere repulsion forces from the long-ranged electrostatic interaction and the translational Brownian movement.

Experimental

Materials

Four kinds of fluorine-containing polymer spheres, i.e., poly(tetrafluoroethylene) (PTFEA, diameter 130 nm), poly(tetrafluoroethylene) (PTFEB, 210 nm), copolymer of tetrafluoroethylene and perfluorovinylether (PFA, 120 nm) and copolymer of tetrafluoroethylene and perfluoropropylene(10%) (PTP, 130 nm) were used. Their diameters were estimated from dynamic light scattering measurements in the presence of sodium chloride at 10^{-4} mol/l. Their densities were estimated to be 2.3, 2.2, 2.2 and 2.2, respectively. These stock suspensions were deionized exhaustively with mixed beds of cation- and anion-exchange resins [AG501-X8(D), 20–50 mesh, Bio-Rad Lab., Hercules, Calif.] for more than 1 year in Pyrex glass bottles shielded as completely as possible. The colloidal sample suspension was prepared in a test tube (disposable culture tube, borosilicate glass, Corning Glass Works, Corning, N.Y., 11 and 13 mm inside and outside diameters) shielded tightly with Parafilm (American Can Co., Greenwich, Conn.). The suspensions were treated with a small amount of the Bio-Rad resins for several days in the tube with gentle inverted mixing several times a day.

The water used for the sample preparation was purified using a Milli-Q reagent grade system (Milli-RO5 plus and Milli-Q plus, Millipore Co., Bedford, Mass.).

Closeup colour photography

The photographing of the colloidal crystals in a test tube was done with a Canon EOS10 camera, a macro lens (EF50 mm, $f = 22$) and a life-size converter (EF). Vervia film (Fujichrome, RVP 135, ISO = 50) was used for colour transparencies. The light source was a pocket-type flashlight (BF-775, Xenon 4, National, Osaka), which is weak enough to prevent thermal destruction of the single crystals and contains plenty of reddish (long-wavelength) light resulting in beautiful pictures.

Reflection spectroscopy

The reflection spectra at an incident angle of 90° were recorded on a multi-channel photodetector (MCPD-110B, Otsuka Electronics, Hirakata, Osaka) connected to a Y-type optical fibre cable. The instrument was operated by a microcomputer (MC800, Otsuka Electronics).

Results and discussion

Giant single crystals formed in the exhaustively deionized suspensions

A closeup colour photograph of the single crystals formed for an exhaustively deionized aqueous suspension of PTFEB 9 days after suspension preparation in a test tube is shown in Fig. 1. The picture was taken 1 day after vertical mixing and standing still on a table. The specific gravity of the spheres was very high compared with that of the solvent, and significant sedimentation took place even after 1 day. The sphere concentration at the height where a giant single crystal is seen in the figure was 0.0008 in volume fraction. The sphere concentration was determined from the peak wavelength in the reflection spectra. A very large single crystal, about 5 mm, is seen in the figure. The change in colour from bluish to reddish is due to the change in the incident angle of light through the curved wall of the test tube. These patterns of the single crystals changed rapidly

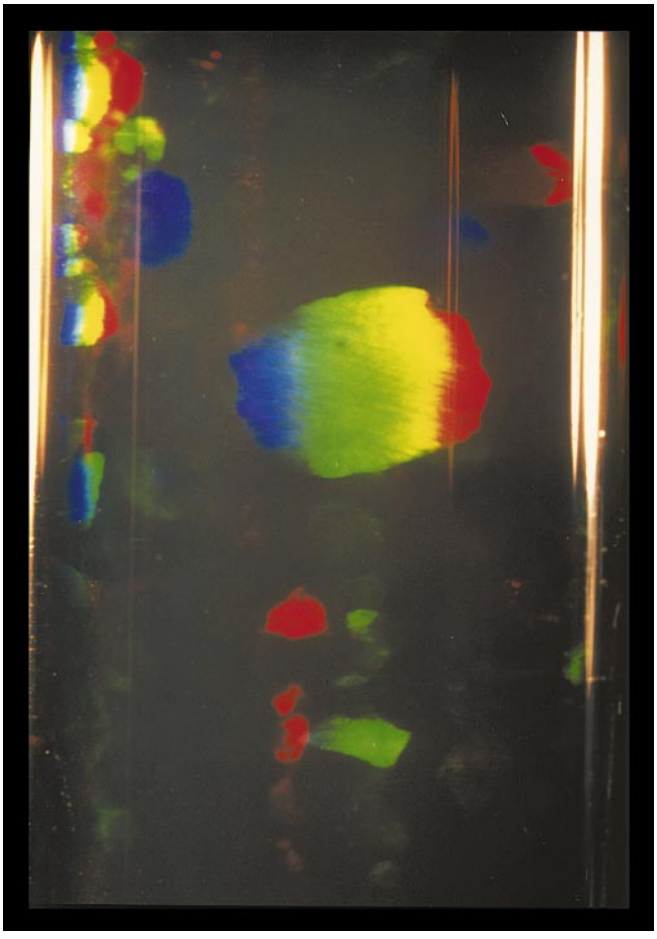

Fig. 1 Closeup picture of poly(tetrafluoroethylene)B (*PTFEB*) suspension with resins at 25 °C. 9 days after suspension preparation, $\phi = 0.0008$. The picture was taken 1 day after vertical mixing. Exposure = 1/3 s, iris = 22

with a very slow rotation of the test tube. Two kinds of single crystals are observed, very large blocklike crystals and pillarlike ones. The former appear in the bulk phase far from the cell wall and grow by homogeneous nucleation. On the other hand, the latter are from heterogeneous nucleation along the cell wall. The shapes of the former were quite varied. Triangle, cubiclike, pentagonal, hexagonal and even conelike single crystals were observed. The single crystals were packed densely and void regions were never observed; this is supported by the change of the patterns of the single crystals when the test tube was rotated very slowly. In this figure the background is very dark, but the suspension is full of single crystals surrounded by grain boundaries. The suspensions and the single crystals of the fluorine-containing spheres were more transparent than those of colloidal silica and polystyrene spheres. This may be due to the fact that the refractive indices of the former (e.g. 1.35 at room temperature for PTFE) are closer to that of water (1.33 at 25 °C). For comparison, the refractive indices of silica and polystyrene are reported to be about 1.5 and 1.60, respectively.

The single crystals formed for the suspensions of PFA containing sodium chloride (3×10^{-7} mol/l) 3 minutes after vertical mixing are shown in Fig. 2. The initial sphere volume fraction was 0.003 in volume fraction. Many crystals around 2 mm in size formed by homogeneous nucleation are seen packed densely in the whole of the suspension.

Phase diagram

The phase diagrams of colloidal crystals of PTFEA, PTFEB, PFA and PTP in the exhaustively deionized aqueous suspensions are shown in Fig. 3. The open and solid circles show the crystal-like and liquidlike phases. The critical sphere concentrations of melting, ϕ_c were

Fig. 2 Closeup picture of a suspension of copolymer of tetrafluoroethylene and perfluorovinylether (*PFA*) with sodium chloride (3×10^{-7} M) at 25 °C. $\phi^* = 0.003$. The picture was taken 3 min after vertical mixing. Exposure = 3 s, iris = 22

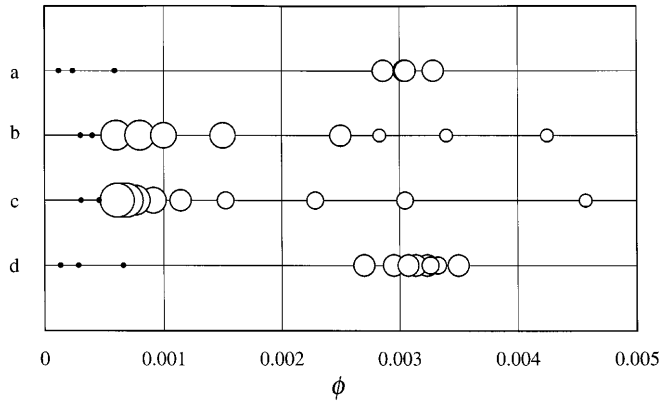

Fig. 3 Phase diagram of PTFEA (*a*), PTFEB (*b*), PFA (*c*) and PTP (*d*) suspensions with resins at 25 °C. *Large open circles*: size of single crystal is larger than 3 mm; *medium-sized circles*: 0.5–3 mm; *small circles*: smaller than 0.5 mm; *very small filled circles*: liquid state

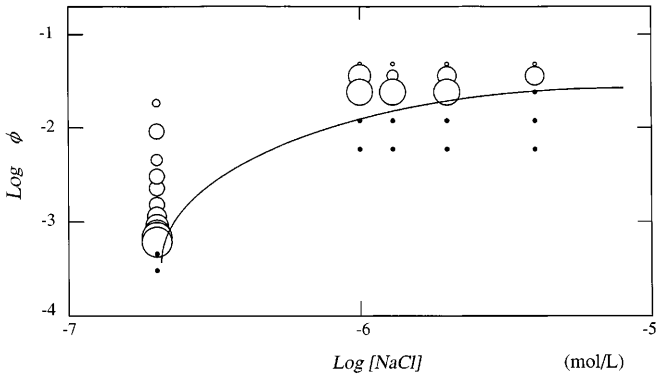

Fig. 4 Phase diagram of PFA suspensions with sodium chloride at 25 °C. *Very large open circles*: size of single crystal is larger than 3 mm; *large circles*: 1.5–3 mm; *medium-sized circles*: 0.7–1.5 mm; *small circles*: smaller than 0.7 mm; *very small circles*: smaller than 0.2 mm; *very small filled circles*: liquid state

estimated to be around 0.0006 in volume fraction. This value was close to, but clearly slightly larger than, those of polystyrene spheres ($\phi_c \approx 0.00015$) and colloidal silica spheres (0.0002–0.0004). These differences are ascribed to the following facts. First, the colloidal spheres of the fluorine-containing polymer spheres used in this work are rather polydisperse compared with polystyrene and silica spheres. Second, fluorine-containing polymers are highly hydrophobic and not so stable with respect to aggregation, especially at the air–suspension and glass–suspension interfaces; however, the morphology of the single crystals of the fluorine-containing colloidal spheres was quite similar to that of polystyrene and/or silica spheres. The size of the single crystals was largest at a sphere concentration slightly higher than the critical sphere concentration of melting and decreased as the sphere concentration increased.

The phase diagram of PFA suspensions in the presence of sodium chloride is shown in Fig. 4. The data at the lowest concentration of sodium chloride of 2×10^{-7} mol/l are the ones for the exhaustively deionized suspensions with the resins. It is interesting to note that large single crystals (1.5–3 mm) are formed even in the presence of up to 5×10^{-6} mol/l sodium chloride.

Reflection spectroscopy in sedimentation equilibrium and the elastic moduli of colloidal crystals

A closeup colour photograph of the single crystals of PTFEA in sedimentation equilibrium is shown in Fig. 5. It is clear that many single crystals, 1–2 mm in size, are packed densely throughout the suspension. The suspension was kept still on a desk for 1 month. In the reflection measurements the incident white light hits the surface of the sample cell at right angles. When the cell contains an "ordered" colloidal suspension the light is turned back by Bragg diffraction. This corresponds to the reflection spectrum shown in Fig. 6. Generally speaking, the shape of a reflection-spectrum pattern is a single peak, a double peak or a single peak with a shoulder. The two-wavelength peaks were always close together, with a difference of only 1.03 in the ratios of their wavelengths. This difference supports the idea that the peak appearing at the longer wavelength may be ascribed to the face-centred-cubic (fcc) lattice and the shorter-wavelength peak corresponds to the body-centred-cubic (bcc) lattice in the crystal structures. Using a simple theoretical calculation, the ratio of the nearest-neighbour Bragg distance for fcc lattices to that for bcc ones was found to be 1.028 at the same sphere concentration. The intersphere spacing observed (D) was determined from the peak wavelength. For both fcc and bcc lattices the distance (D_{fcc} or D_{bcc}) at a scattering angle of 90° is given by

$$D_{fcc} = D_{bcc} = 0.6124(\lambda_m/n_s) \quad , \tag{1}$$

where n_s is the refractive index of the sphere suspension (taken as that of water in this work) and λ_m is the peak wavelength. The fcc distribution was stable at higher sphere concentrations than the bcc structure. The highest reflection peaks in the figure were secondary ones from the Bragg reflection; this was clarified by comparison of the primary peak wavelengths calculated from the initial sphere concentration and the observed peak wavelengths. The initial sphere concentration, ϕ^*, was 0.00325. Clearly, the size of the crystals in the higher layers was larger, which corresponds to the fact that the sphere concentration decreases as the height increases. The number of the reflection spectra in Fig. 6 corresponds to the number code with an arrow in Fig. 5.

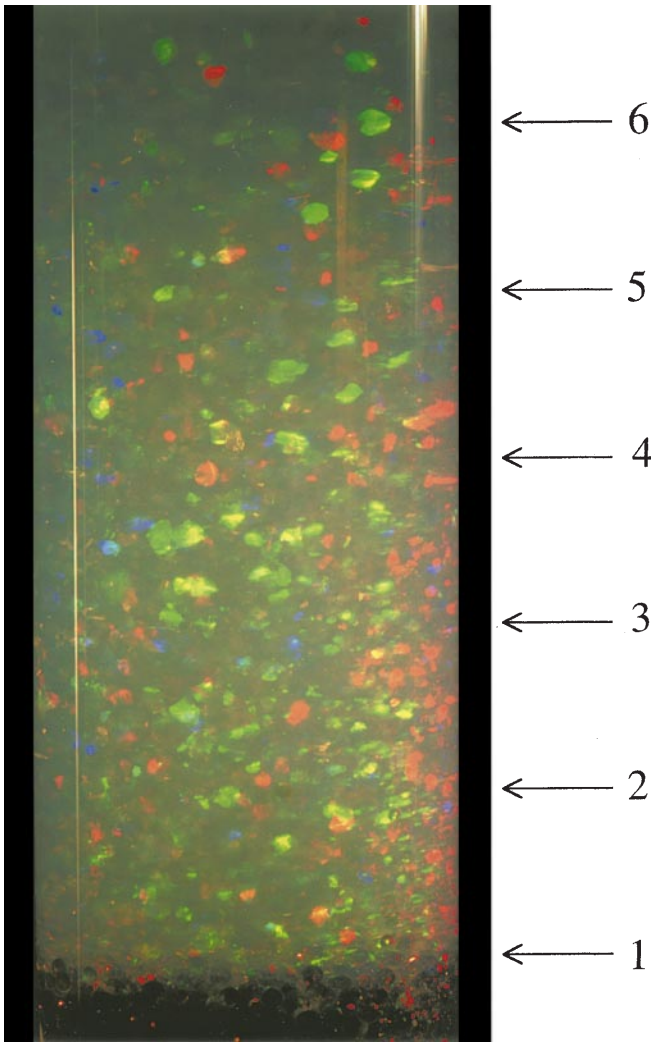

Fig. 5 Closeup picture of PTFEA suspensions with resins at 25 °C 29 days after suspension preparation, $\phi^* = 0.00325$. The picture was taken 26 days after vertical mixing. Exposure = 1/3 s, iris = 22. *Bars 1–6* in the picture show the locations where the reflection spectra were taken in Fig. 6

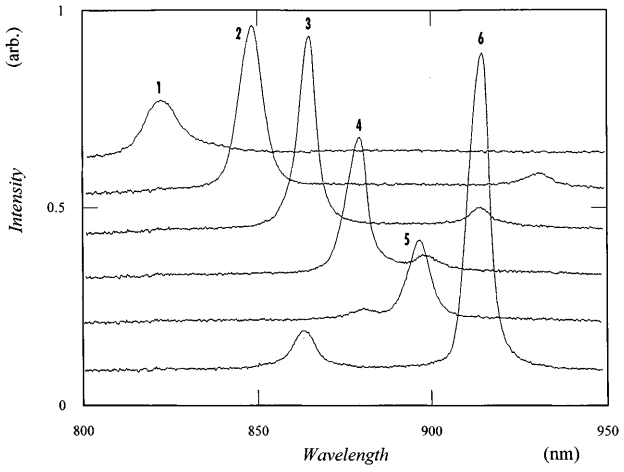

Fig. 6. Reflection spectra of PTFEA suspension with resins at 25 °C. 29 days after suspension preparation, $\phi^* = 0.00325$. The spectra were taken 26 days after setting the suspension

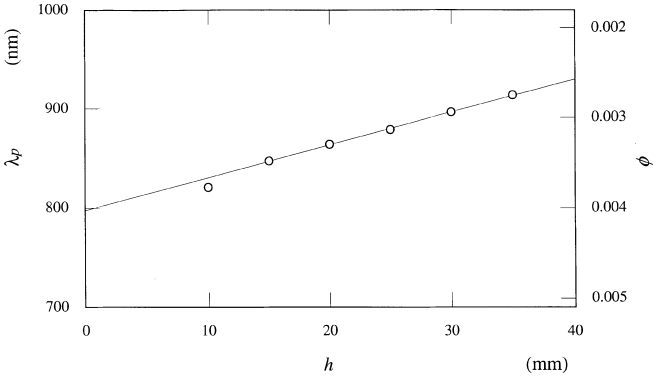

Fig. 7. Changes in λ_p and ϕ of PTFEA suspension with resins at various heights. 26 days after setting the suspension, $\phi^* = 0.00325$

According to Crandall and Williams [26], the peak wavelength, λ_p, in sedimentation equilibrium is given by

$$\lambda_p - \lambda_m = (\rho_{eff} g_0 \lambda_m \phi_m / G)(h - h_m) \ , \qquad (2)$$

where h and h_m are the heights of the horizontal plane examined and the horizontal midplane of the colloidal suspension in the cell. λ_m and ϕ_m indicate the peak wavelength and the sphere concentration in volume fraction at the midplane, respectively. ϕ_m is, therefore, equal to a ϕ^* of 0.00325. ρ_{eff} is the effective density given by the specific gravity of the sphere minus that of the solvent, and g_0 is the gravitational constant. Thus, the elastic modulus, G, is evaluated from the slope of the λ_p versus h plots in Fig. 7. The right-hand-side ordinate, ϕ, was calculated from the λ_p value: the linear relationship was excellent. The G value of PTFEA was 10.8 Pa at N (number of spheres per unit volume) $= 3.53 \times 10^{13}$ cm^3. The G value of PTP was also obtained to be 28.7 Pa at $N = 3.50 \times 10^{13}$ cm^{-3}, though the relevant graphs are omitted here.

A theoretical discussion on the elastic modulus of colloidal crystals has been made by several researchers [27–31]. The order of magnitudes of the modulus may be written in terms of the magnitude of the thermal fluctuation, δ, of a sphere as

$$G = f/D = (k_B T / \langle d^2 \rangle)/D \ , \qquad (3)$$

where f is the force constant, D is the intersphere distance, δ is the thermal fluctuation of a sphere in the effective potential valley, k_B is the Boltzmann constant and T is the temperature. Introducing a nondimensional parameter, g, for $\langle d^2 \rangle^{1/2}/D$, the modulus is obtained as a linear function of N

$$G = Nk_{\mathrm{B}}T/g^2 \quad . \tag{4}$$

When $g = 1$, Eq. (4) gives the elastic modulus of an ideal gas having the same sphere concentration. Lindemann's law of crystal melting tells us that $g < 0.1$ holds for a stable crystal. The g values were evaluated using Eq. (4) to be 0.116 and 0.071 for PTFEA and PTP, respectively. Thus, these crystals may be not so stable.

Conclusions

It is clear from this work that colloidal crystals are formed even for highly hydrophobic colloidal spheres of fluorine-containing polymer spheres. As described in the Introduction, intersphere repulsion forces, from the electrostatic repulsion of the expanded electrical double layers especially in the deionized system and also from the thermal fluctuation of colloidal spheres themselves, are essential for colloidal crystallization. These repulsion forces are long-ranged compared with the hydrophobic forces. Thus, the colloidal crystallization of the fluorine-containing spheres in this work suggests that colloidal crystals are formed by the intersphere repulsion forces exclusively and that the formation is quite independent of the nature of the colloidal spheres.

Acknowledgements Financial support from the Ministry of Education, Science, Sports and Culture, Japan, Grants-in-aid for Scientific Research on Priority Areas(A) 11167241 and for Scientific Research(B) 11450367 is gratefully acknowledged.

References

1. Vanderhoff W, van de Hul HJ, Tausk RJM, Overbeek JThG (1970) In: Goldfinger G (ed) Clean surfaces: their preparation and characterization for interfacial studies. Dekker, New York, p 15
2. Hiltner PA, Papir YS, Krieger IM (1971) J Phys Chem 75:1881
3. Kose A, Ozaki M, Takano K, Kobayashi Y, Hachisu S (1973) J Colloid Interface Sci 44:330
4. Williams R, Crandall RS, Wojtowicz PJ (1976) Phys Rev Lett 37:348
5. Mitaku S, Ohtsuki T, Enari K, Kishimoto A, Okano K (1978) Jpn J Appl Phys 17:305
6. Lindsay HM, Chaikin PM (1982) J Chem Phys 76:3774
7. Pieranski P (1983) Contemp Phys 24:25
8. Ottewill RH (1985) Ber Bunsenges Phys Chem 89:517
9. Aastuen DJW, Clark NA, Cotter LK, Ackerson BJ (1986) Phys Rev Lett 57:1733
10. Pusey PN, van Megen W (1986) Nature 320:340
11. Okubo T (1988) Acc Chem Res 21:281
12. van der Koo FM, Lekkerkerker HNW (1998) J Phys Chem B 102:7829
13. Liu L, Li P, Asher SA (1999) J Am Chem Soc 121:4040
14. Ackerson BJ, Clark NA (1981) Phys Rev Lett 46:123
15. Lowen H, Palberg T, Simon R (1993) Phys Rev Lett 70:1557
16. Okubo T (1994) In: Schmitz KS (ed) Macro-ion characterization. From dilute solutions to complex fluids. ACS Symposium Series 548. American Chemical Society, Washington, D.C., p 364
17. Pusey PN, van Megen W (1987) In: Safran SA, Clark NA (eds) Complex and supramolecular fluids. Wiley-Interscience, New York, p 673
18. Russel WB (1990) Phase Transitions 21:127
19. Dhont JKG, Smits C, Lekkerkerker HNW (1992) J Colloid Interface Sci 152:386
20. Schatzel K, Ackerson BJ (1993) Phys Rev E 48:3766
21. Butler S, Harrowell P (1995) Phys Rev E 52:6424
22. Okubo T (1994) Langmuir 10:1695
23. Okubo T (1992) Naturwissenschaften 79:317
24. Okubo T (1993) Colloid Polym Sci 271:190
25. Itano WM, Bolinger JJ, Tan JN, Jelenkovic B, Huang XP, Wineland DJ (1998) Science 279:686
26. Crandall RS, Williams R (1977) Science 198:293
27. Mitaku S, Ohtsuki T, Okano K (1978) Jpn J Appl Phys 17:305; 627
28. van Megen WJ, Snook IK, Watts RO (1980) J Colloid Interface Sci 77:131
29. Russel WB, Benzing DW (1981) J Colloid Interface Sci 83:163
30. Buscall R, Goodwin JW, Hawkins MW, Ottewill RH (1982) J Chem Soc Faraday Trans 178:2889
31. Lindsay HM, Dozier WD, Chaikin PM, Klein R, Hess W (1986) J Phys A 19:2583